various bands are given by

$$E_j^n = \frac{V_0}{2} + \frac{\pi^2\hbar^2[1+(\beta/m)\delta^2]}{2ma^2}\, n^2 + \frac{ma^2V_0^2}{16\pi^2\hbar^2(1+\beta\delta^2/m)(n^2-1)} + OV_0^4 . \quad (76)$$

Substituting for E and δ one finds

$$h\nu_{\text{free}} = \frac{V_0}{2} + \frac{\pi^2\hbar^2n^2}{2ma^2} + \frac{8\beta k^2a^2}{n^2} + OV_0^2 . \quad (77)$$

This last equation is not very helpful since it gives the energies or frequencies associated with the band edges (i.e., the tops and bottoms of the bands), but for energies much larger than V_0 the bands are very wide.

The wave functions described have equal probabilities for the jth atom to be in any valley. To describe localized particles it would be necessary to construct wave packets made up of Mathieu functions. We will leave such treatments for a later paper.

The treatment given depends in a very important way on our ability to make a convergent expansion of the displacement in terms of time derivatives. It is not enough to say that x_{j+1} is the same as x_j except for a phase factor. Such a procedure does not allow the harmonic forces to be described in terms of an effective mass. Such a procedure generates separable but complicated equations of motion.

---

†Research supported by Army Research Office, Durham, under Contract No. DA-31-124-ARO(D)-65.

[1]J. Frenkel and T. Kontorova, Physik Z. Sowjet Union 13, 1 (1938).

[2]E. Jahnke and F. Emde, *Tables of Functions*, 4th ed. (Dover, New York, 1945), pp. 52 and 92.

[3]Reference 2, p. 73.

[4]P. F. Byrd and M. D. Friedman, *Handbook of Elliptic Functions for Engineers and Physicists* (Springer, Berlin, 1954), p. 8.

[5]Reference 2, p. 283; see also M. Abramowitz and I. A. Stegun, *Handbook of Mathematical Functions* (Dover, New York, 1965), p. 722.

PHYSICAL REVIEW B VOLUME 4, NUMBER 6 15 SEPTEMBER 1971

Lattice Dynamics of Transition Metals—Application to Paramagnetic Nickel

Satya Prakash and S. K. Joshi
Physics Department, University of Roorkee, Roorkee, India
(Received 30 November 1970)

The problem of lattice dynamics of transition metals is investigated. For the case of paramagnetic nickel, the isotropic two-band model is used to evaluate the static dielectric function in the Hartree approximation. The bare-ion potential is represented by a two-parameter model potential. The phonon frequencies are calculated for the configurations $(3d)^9(4s)^1$ and $(3d)^{9.4}(4s)^{0.6}$, and compared with the experimental measurements along the three principal symmetry directions [100], [110], and [111]. A fairly good agreement is obtained for both configurations.

I. INTRODUCTION

A good deal of work has been done on the lattice dynamics of normal metals and we have a fairly satisfactory understanding of phonons in these metals.[1–4] The problem of lattice dynamics of transition metals is interesting but characteristically difficult. In these metals the distinction between the core and the conduction electron is not clear. The outermost d shell is not completely filled and the electronic-band-structure calculations[5] show that the wave functions of the conduction electrons have a strong d character. Thus the d states are not sufficiently tightly bound and it is not valid to treat them in the same way as in the case of free atoms. Harrison[6] approached this problem by generalizing the pseudopotential formulation to include the d states in the transition metals. The pseudopotential obtained by him includes the effects of s-d hybridization but is nevertheless weak. The pseudopotential approach for transition metals has not yet been utilized for developing a theory of lattice vibrations in these metals. Sinha[7] and Golibersuch[8] have independently studied the electron-phonon interaction in transition metals using the augmented-plane-wave method. Because of the complexities of these approaches, actual calculations for any metal have not been attempted as yet.

Recently, the authors[9] proposed a noninteracting band model to calculate the static dielectric function of the transition metals (hereafter we refer to this paper as I). The free-electron approximation is used for the electrons in the s band, while

a simplified tight-binding scheme is used for the d electrons. The electronic energies are assumed to be given by the effective-mass approximation. The scheme is applied to paramagnetic nickel and it is found that the major contribution to the dielectric function is due to intraband transitions. The contribution from the electrons in the unfilled d band dominates. In this paper we propose a method for studying the lattice dynamics of the transition metals assuming the presence of both the d-like and s-like conduction electrons. We use this formulation to calculate the phonon frequencies of paramagnetic nickel.

In Sec. II, we start from the Hartree-Fock approximation for the electronic ground-state energy and derive an expression for the second-order change in energy which involves the screened electron-phonon matrix element. The explicit expressions for the electron-phonon matrix element and the static dielectric matrix are also derived. This enables us to obtain an expression for the electronic contribution to the dynamical matrix. The descriptions of the two-band model for the static dielectric function and the parametrized model potential are also given. The procedure of the calculations and the results are presented in Sec. III. In Sec. IV, we discuss the results.

II. THEORY

A. Electronic Contribution to Dynamical Matrix

In the harmonic approximation, the angular frequencies ω_{qp} of lattice vibrations of a monatomic metal are obtained from the solution of the determinantal equation

$$\det\left|D_{\alpha\beta}(\vec{q}) - M\omega_{qp}^2\,\delta_{\alpha\beta}\right| = 0 \ . \tag{1}$$

Here $\vec{q}$ is the phonon wave vector, p is the polarization branch, M is the mass of the ion, $D_{\alpha\beta}(\vec{q})$ are the elements of the dynamical matrix, and α, β are the Cartesian components (x, y, z). For metallic crystals, the contribution to the dynamical matrix is separated into three parts[1]: (i) the Coulomb interaction between the ions, (ii) the exchange overlap interaction between the ions, and (iii) the ion-electron–ion interaction which also includes electron-electron interaction. Contribution (i) is evaluated in a straightforward manner with the help of Ewald's[10] θ-function transformation, if the charge of the ions and the crystal structure are known. We neglect contribution (ii) assuming that the overlap between the cores is small. Therefore, the main problem is to evaluate the electronic contribution to the dynamical matrix.

A derivation of the electronic contribution to the dynamical matrix in the Hartree approximation is given in Ref. 1. In simple metals the conduction electrons are allocated to a single nearly free-electron-like band, while in transition metals, noble metals, and rare earths, the conduction electrons exhibit both s-like and d-like character.[5] The magnetic behavior of these metals is also quite important and can be studied by using a spin-dependent Hamiltonian. For the sake of simplicity we limit ourselves here to paramagnetic and nonmagnetic systems and disregard the explicit spin dependence of the Hamiltonian.

If we introduce the band indices in the eigenvalues and eigenfunctions for conduction electrons and evaluate the change in the ground-state energy of the electron-ion system up to second order in ion displacements, we get[1]

$$\begin{aligned} E_0^{(2)} = \frac{1}{2} \sum_{lmkl'm'k'}{}' \frac{n_{lm}(\vec{k}) - n_{l'm'}(\vec{k}')}{E_{lm}^{(0)}(\vec{k}) - E_{l'm'}^{(0)}(\vec{k}')} \\ \times \langle \psi_{lmk}^{(0)}(\vec{r}) \left| H_e^{(1)}(\vec{r}) \right| \psi_{l'm'k'}^{(0)}(\vec{r}) \rangle \\ \times \langle \psi_{l'm'k'}^{(0)}(\vec{r}) \left| V_b^{(1)}(\vec{r}) \right| \psi_{lmk}^{(0)}(\vec{r}) \rangle \\ + \sum_{lmk} n_{lm}(\vec{k}) \langle \psi_{lmk}^{(0)}(\vec{r}) \left| V_b^{(2)}(\vec{r}) \right| \psi_{lmk}^{(0)}(\vec{r}) \rangle \ . \end{aligned} \tag{2}$$

Here the superscripts denote the order of perturbation in the ionic displacements. $\psi_{lmk}(\vec{r})$ is the eigenfunction corresponding to the orbital quantum number l, magnetic quantum number m, and wave vector $\vec{k}$, and $E_{lm}(\vec{k})$ is the corresponding eigenvalue. $n_{lm}(\vec{k})$ is the Fermi occupation probability function. $H_e(\vec{r})$ is the electronic Hamiltonian, and $V_b(\vec{r})$ is the electron-ion potential. The prime on $\sum'$ denotes that the term $l=l'$, $m=m'$, and $\vec{k}=\vec{k}'$ is to be omitted. The electron wave vectors $\vec{k}$ and $\vec{k}'$ satisfy the momentum-conservation condition

$$\vec{k}' = \vec{k} - \vec{q} \pm \vec{H} \ ,$$

where $\vec{H}$ is the reciprocal-lattice vector.

On the right-hand side of Eq. (2), the first term represents a repeated one-phonon process, while the second term corresponds to an intrinsic two-phonon process. There are two types of matrix elements in the first term:

$$\langle \psi_{lmk}^{(0)}(\vec{r}) \left| H_e^{(1)}(\vec{r}) \right| \psi_{l'm'k'}^{(0)}(\vec{r}) \rangle$$

is the electron-phonon matrix element while

$$\langle \psi_{l'm'k'}^{(0)}(\vec{r}) \left| V_b^{(1)}(\vec{r}) \right| \psi_{lmk}^{(0)}(\vec{r}) \rangle$$

is the bare-electron–ion matrix element. We follow the general procedure outlined by Sham and Ziman[11] to set up a relationship between these two matrix elements and find

$$\langle\psi^{(0)}_{l'm'k'}(\vec{r})\,|\,H^{(1)}_{eqp\alpha}(\vec{r})\,|\,\psi^{(0)}_{lmk}(\vec{r})\rangle - \sum_{l_1m_1k_1}\sum_{l_2m_2k_2}{}' \frac{n_{l_1m_1}(\vec{k}_1)-n_{l_2m_2}(\vec{k}_2)}{E^{(0)}_{l_1m_1}(\vec{k}_1)-E^{(0)}_{l_2m_2}(\vec{k}_2)}$$

$$\times\langle\psi^{(0)}_{l_2m_2k_2}(\vec{r})\,|\,H^{(1)}_{eqp\alpha}(\vec{r})\,|\,\psi^{(0)}_{l_1m_1k_1}(\vec{r})\rangle\,(v_{k'k_1k_2k}-\overline{V}_{k'k_1k_2k})$$

$$=\langle\psi^{(0)}_{l'm'k'}(\vec{r})\,|\,V^{(1)}_{bqp\alpha}(\vec{r})\,|\,\psi^{(0)}_{lmk}(\vec{r})\rangle\ , \tag{3}$$

where

$$v_{k'k_1k_2k}=\iint\psi^{(0)*}_{l'm'k'}(\vec{r})\,\psi^{(0)*}_{l_1m_1k_1}(\vec{r}')\,\frac{e^2}{|\vec{r}-\vec{r}'|}\,\psi^{(0)}_{l_2m_2k_2}(\vec{r}')\,\psi^{(0)}_{lmk}(\vec{r})\,d^3r\,d^3r'\ , \tag{4}$$

$$\overline{V}_{k'k_1k_2k}=\iint\psi^{(0)*}_{l'm'k'}(\vec{r})\,\psi^{(0)*}_{l_1m_1k_1}(\vec{r}')\,\frac{e^2}{2|\vec{r}-\vec{r}'|}\,\psi^{(0)}_{l_2m_2k_2}(\vec{r})\,\psi^{(0)}_{lmk}(\vec{r}')\,d^3r\,d^3r'\ . \tag{5}$$

Here $V^{(1)}_{bqp\alpha}(\vec{r})$ and $H^{(1)}_{eqp\alpha}(\vec{r})$ are the α components of the Fourier expansion coefficients of $V^{(1)}_b(\vec{r})$ and $H^{(1)}_e(\vec{r})$, respectively, for the phonon of the wave vector $\vec{q}$ and the polarization p. $v_{k'k_1k_2k}$ and $\overline{V}_{k'k_1k_2k}$ are the conduction electron Coulomb and exchange potentials, respectively. The nonlocal nature of exchange potential makes the problem intractable. In I we completely neglected the exchange term in our treatment of the static dielectric function. In this calculation of phonon frequencies also, we shall neglect these effects and restrict ourselves to the Hartree approximation.

It is possible to transform Eq. (3) to the following form:

$$V^{(1)}_{bqp\alpha}(\vec{q}+\vec{G})=\textstyle\sum_{G'}\epsilon(\vec{q}+\vec{G},\vec{q}+\vec{G}')\,H^{(1)}_{eqp\alpha}(\vec{q}+\vec{G}')\ , \tag{6}$$

where $V^{(1)}_{bqp\alpha}(\vec{q}+\vec{G})$ and $H^{(1)}_{eqp\alpha}(\vec{q}+\vec{G})$ are the Fourier transforms of $V^{(1)}_{bqp\alpha}(\vec{r})$ and $H^{(1)}_{eqp\alpha}(\vec{r})$, respectively. $\vec{G}$ is the reciprocal-lattice vector and the dielectric matrix $\epsilon(\vec{q}+\vec{G},\vec{q}+\vec{G}')$ is given by

$$\epsilon(\vec{q}+\vec{G},\vec{q}+\vec{G}')$$

$$=\delta_{GG'}-v(\vec{q}+\vec{G})\sum_{l_1m_1k_1}\sum_{l_2m_2k_2}{}'\frac{n_{l_1m_1}(\vec{k}_1)-n_{l_2m_2}(\vec{k}_2)}{E^{(0)}_{l_1m_1}(\vec{k}_1)-E^{(0)}_{l_2m_2}(\vec{k}_2)}$$

$$\times\langle\psi^{(0)}_{l_1m_1k_1}(\vec{r})\,|\,e^{-i(\vec{q}+\vec{G})\cdot\vec{r}}\,|\,\psi^{(0)}_{l_2m_2k_2}(\vec{r})\rangle$$

$$\times\langle\psi^{(0)}_{l_2m_2k_2}(\vec{r})\,|\,e^{i(\vec{q}+\vec{G}')\cdot\vec{r}}\,|\,\psi^{(0)}_{l_1m_1k_1}(\vec{r})\rangle\ , \tag{7}$$

where

$$v(\vec{q}+\vec{G})=4\pi e^2/\Omega_0|\vec{q}+\vec{G}|^2\ , \tag{8}$$

where Ω_0 is the atomic volume.

The electron-phonon matrix element can now be expressed in terms of the bare-electron–ion matrix element

$$\langle\psi_{l'm'k'}(\vec{r})\,|\,H^{(1)}_{eqp\alpha}(\vec{r})\,|\,\psi^{(0)}_{lmk}(\vec{r})\rangle$$

$$=\sum_G\sum_{G'}\epsilon^{-1}(\vec{q}+\vec{G},\vec{q}+\vec{G}')\,V^{(1)}_{bqp\alpha}(\vec{q}+\vec{G}')$$

$$\times\langle\psi^{(0)}_{l'm'k'}(\vec{r})\,|\,e^{i(\vec{q}+\vec{G})\cdot\vec{r}}\,|\,\psi^{(0)}_{lmk}(\vec{r})\rangle\ . \tag{9}$$

The second term on the right-hand side of Eq. (2) will contribute only when $\vec{q}=0$ or $\vec{q}=\vec{H}$. $\vec{q}$ is a vector in the first Brillouin zone and cannot equal $\vec{H}$; and $\vec{q}=0$ is consistently dropped in our treatment in order to satisfy the charge neutrality condition. Thus, this term in Eq. (2) does not contribute to $E^{(2)}_0$ and we can write

$$E^{(2)}_0=\frac{1}{2}\sum_{lmkl'm'k'}{}'\frac{n_{lm}(\vec{k})-n_{l'm'}(\vec{k}')}{E^{(0)}_{lm}(\vec{k})-E^{(0)}_{l'm'}(\vec{k}')}\sum_{qp\alpha q'p'\beta}\sum[a_{qp}a_{q'p'}]$$

$$\times\sum_G\sum_{G'}\epsilon^{-1}(\vec{q}+\vec{G},\vec{q}+\vec{G}')\,V^{(1)}_{bqp\alpha}(\vec{q}+\vec{G}')\,\langle\psi^{(0)}_{lmk}(\vec{r})\,|\,e^{i(\vec{q}+\vec{G})\cdot\vec{r}}\,|\,\psi_{l'm'k'}(\vec{r})\rangle$$

$$\times\sum_{G''}V^{(1)}_{bq'p'\beta}(\vec{q}'+\vec{G}'')\,\langle\psi^{(0)}_{l'm'k'}(\vec{r})\,|\,e^{i(\vec{q}'+\vec{G}'')\cdot\vec{r}}\,|\,\psi^{(0)}_{lmk}(\vec{r})\rangle\ , \tag{10}$$

where a_{qp} is the amplitude of vibrations for the qth mode and pth branch.

Assuming the dielectric matrix to be diagonal as we did in I, and using the momentum-conservation conditions for the nonvanishing matrix elements, Eq. (10) simplifies to

$$E_0^{(2)} = \frac{1}{2}\sum_q \sum_{p,p'} \sum_{\alpha,\beta} \sum_G \epsilon^{-1}(\vec{q}+\vec{G})\,\chi(\vec{q}+\vec{G}) \times [a_{qp} a^*_{qp'} V^{(1)}_{bqp\alpha}(\vec{q}+\vec{G})\, V^{(1)*}_{bqp'\beta}(\vec{q}+\vec{G})] \,. \quad (11)$$

Here $\chi(\vec{q}+\vec{G})$ is defined by the relation

$$\epsilon(\vec{q}+\vec{G}) = 1 - v(\vec{q}+\vec{G})\,\chi(\vec{q}+\vec{G}) \,. \quad (12)$$

Substituting explicit expressions for $V^{(1)}_{bqp\alpha}(\vec{q}+\vec{G})$ into (11) we obtain

$$E_0^{(2)} = \frac{1}{2}\sum_q \sum_{p,p'} \sum_{\alpha,\beta} e_{qp\alpha}\, e_{qp'\beta}\, a_{qp} a^*_{qp'} \sum_G \bar{D}_{\alpha\beta}(\vec{q}+\vec{G}) \,, \quad (13)$$

where $\vec{e}_{qp\alpha}$ is the α component of the unit polarization vector $\vec{e}_{qp}$ and

$$\bar{D}_{\alpha\beta}(\vec{q}+\vec{G}) = (N/M)\,\epsilon^{-1}(\vec{q}+\vec{G}) \times \chi(\vec{q}+\vec{G})(\vec{q}+\vec{G})_\alpha (\vec{q}+\vec{G})_\beta |\, U_b(\vec{q}+\vec{G})\,|^2 \,. \quad (14)$$

N is the number of unit cells in the crystal and $U_b(\vec{q}+\vec{G})$ is the Fourier transform of single-ion potential seen by a conduction electron. Therefore, the electronic contribution to the phonon frequencies is

$$\omega^2_{qp}(E) = \sum_{\alpha,\beta} \left(\sum_G \bar{D}_{\alpha\beta}(\vec{q}+\vec{G}) - \sum_{G\neq 0} \bar{D}_{\alpha\beta}(\vec{G}) \right) e^*_{qp\alpha}\, e_{qp\beta} \,. \quad (15)$$

With the use of Eqs. (12) and (14) this simplifies to

$$\omega^2_{qp}(E) = \frac{N}{M}\left[\sum_G [\vec{e}_{qp}\cdot(\vec{q}+\vec{G})]^2 \frac{1}{v(\vec{q}+\vec{G})} \left(\frac{1}{\epsilon(\vec{q}+\vec{G})} - 1 \right) |\, U_b(\vec{q}+\vec{G})\,|^2 - \sum_{G\neq 0} (\vec{e}_{qp}\cdot\vec{G})^2 \frac{1}{v(\vec{G})} \left(\frac{1}{\epsilon(\vec{G})} - 1 \right) |\, U_b(\vec{G})\,|^2 \right] . \quad (16)$$

B. Isotropic Two-Band Model

The conduction electrons in a transition metal are distributed in the s and d bands. These electrons respond to the ionic motion through intraband and interband transitions and screen the bare-electron–ion interaction. In I the explicit expression for the dielectric function is written in the form

$$\epsilon(\vec{p}) = 1 - \epsilon_{ss}(\vec{p}) - \epsilon_{dd}(\vec{p}) - \epsilon_{ds}(\vec{p}) - \epsilon_{sd}(\vec{p}) \,, \quad (17)$$

where $\vec{p} = \vec{q}+\vec{G}$. ϵ_{ss}, ϵ_{dd}, ϵ_{ds}, and ϵ_{sd} symbolize the contributions arising from transitions, from s band to s band, d bands to d bands, d bands to s band, and s band to d bands, respectively. In transition metals the s and d bands are admixed owing to s-d interaction. The s and d characters of the wave function in a band vary with $\vec{k}$. It demands heavy computational efforts to use energy bands in a precise manner in the calculation of the dielectric function (17). We, therefore, constructed the noninteracting band model for the specific case of paramagnetic nickel and utilized the band-structure calculations of Hanus.[5] The detailed description and the approximations used in obtaining the noninteracting band model are given in I. ϵ_{dd}, ϵ_{ds}, and ϵ_{sd} are $\vec{k}$ dependent and heavy numerical computations are involved in their evaluation. The use of such a dielectric function for calculating the phonon frequencies even along a few symmetry directions will be a prohibitively difficult task. We, therefore, adopt here a simplified isotropic two-band model to calculate the static dielectric function and the phonon frequencies of nickel.

We find from the Table VI of I that the magnitude of interband contribution ($\epsilon_{ds}+\epsilon_{sd}$) is very small in comparison to the magnitude of the intraband contribution ($\epsilon_{dd}+\epsilon_{ss}$) for the entire region of $\vec{p}$. Therefore, we may justifiably neglect ϵ_{ds} and ϵ_{sd} and retain only intraband transitions. The expression for ϵ_{ss} is

$$\epsilon_{ss}(p) = -\frac{2m_s k_{Fs} e}{\pi\hbar^2 p^2} \left(1 + \frac{4k^2_{Fs} - p^2}{4k_{Fs} p} \ln \left| \frac{2k_{Fs}+p}{2k_{Fs}-p} \right| \right) , \quad (18)$$

where k_{Fs} is the Fermi momentum for the parabolic s band and m_s is the effective mass of the electron for the same band.

The contributions to $\epsilon_{dd}(\vec{p})$ are divided into two parts. In the first part, we have considered the transitions from the unfilled d subband to unfilled d subband and for it $m = m' = 1$. $\epsilon_{dd}(\vec{p})$ for this part is written as

$$\epsilon_{dd}(\vec{p}) = -\frac{2e^2}{\pi\hbar^2 p^2}\, m_{d1} k_{Fd1} |\, \Delta_{21,21}(\vec{p})\,|^2 \times \left(1 + \frac{4k^2_{Fd1} - p^2}{4k_{Fd1} p} \ln \left| \frac{2k_{Fd1}+p}{2k_{Fd1}-p} \right| \right) , \quad (19)$$

where m_{d_1} is the effective mass for $m=1$, d subband; k_{Fd1} is the Fermi momentum for this band assumed to be given by the parabolic approximation for the electron energy and

$$\Delta_{21,21}(\vec{p}) = I_0 - \tfrac{2}{7}(5\pi)^{1/2} Y_2^{(0)*}(\theta_p, \phi_p) I_2 - \tfrac{8}{7}\pi^{1/2} Y_4^{(0)*}(\theta_p, \phi_p) I_4 \ . \quad (20)$$

θ_p, ϕ_p are the polar angles of the vector $\vec{p}$ and the quantities I_0, I_2, and I_4 are explicitly defined in I. Y_l^m are the spherical harmonics. Our calculations have shown the dielectric function to be nearly isotropic. In view of this nearly isotropic behavior, we can simplify our procedure greatly by assuming the vector $\vec{p}$ to lie along the z axis[12] so that $\theta_p = \phi_p = 0$. Substituting for I_0, I_2, and I_4 we get from (20),

$$\Delta_{21,21}(\vec{p}) = 720 \sum_{i,j} a_i a_j \frac{(\alpha_i+\alpha_j)[-7p^2+(\alpha_i+\alpha_j)^2]}{[p^2+(\alpha_i+\alpha_j)^2]^5} \ . \quad (21)$$

Here a_i and α_i are parameters of the $(3d)$-radial wave function and are defined in I.

The second part of $\epsilon_{dd}(\vec{p})$ is due to transitions from the filled d subbands to unfilled d subband. This part vanishes if we take the wave vector $\vec{p}$ along z axis. For $\vec{p}$ along a general direction also, this contribution is very small.[9] The final expression for the dielectric function which we shall use in the calculations of phonon frequencies is then obtained by adding (18) and (19):

$$\epsilon(p) = 1 + \frac{2e^2}{\pi\hbar^2 p^2}\left[m_s k_{Fs}\left(1 + \frac{4k_{Fs}^2 - p^2}{4k_{Fs}p} \ln\left|\frac{2k_{Fs}+p}{2k_{Fs}-p}\right|\right) + m_{d1} k_{Fd1} |\Delta_{21,21}(p)|^2 \left(1 + \frac{4k_{Fd1}^2 - p^2}{4k_{Fd1}p} \ln\left|\frac{2k_{Fd1}+p}{2k_{Fd1}-p}\right|\right)\right] . \quad (22)$$

The dielectric function (22) is independent of $\hat{k}$ and includes the contributions of the intraband transitions in the unfilled s and d bands. It is equivalent to an approximation where the electrons in the completely filled d subbands behave like a tightly bound core and do not respond to the perturbing phonon field. In this model, the ion core will have a $(3d)^8$ configuration for the nickel. The remaining two electrons are assumed to be distributed in the s band and d subband which are not completely filled. We regard that only these two electrons are contributing to the dielectric function (22).

C. Bare-Ion Potential

The model that we have discussed above assumes that we have an ion core with effective charge Ze, where $Z=2$. The bare-ion potential[13,14] is then calculated in the modified Hartree-Fock-Slater self-consistent scheme. In this scheme the Slater exchange potential is replaced by Kohn-Sham[15] exchange potential and correlation corrections are made by using the prescriptions of Robinson *et al.*[16] We neglect the exchange between the core and the conduction electrons. When we use this bare-ion potential to calculate the phonon frequencies in (16) and sum over the reciprocal-lattice vectors $\vec{G}$, $\overline{D}_{\alpha\beta}(\vec{q}+\vec{G})$ does not converge properly. We introduced a damping factor to circumvent the convergence difficulty in (16) but found that even then the phonon frequencies did not come out to be real in all the three principal symmetry directions. This difficulty primarily originates from the fact that the s and d wave functions which we have used are neither mutually orthogonal nor orthogonal to the core wave functions. An explicit orthogonalization of all these functions is a difficult task and would involve $\vec{k}$-dependent coefficients of the wave functions in their combination. We have therefore introduced these corrections by modifying the bare-ion potential to a pseudopotential. We have chosen a model pseudopotential whose Fourier transform is given by[17]

$$U_b(\vec{p}) = -4\pi Ze^2/p^2 + \beta[1+(pr_c)^2]^2 \ . \quad (23)$$

The first term represents the Coulomb potential due to the ionic charge Ze, while the second term represents the repulsive part of the potential. β is the strength of repulsion and parameter r_c is introduced to bring the desired decay of $U_b(\vec{p})$ at large $\vec{p}$. In practice, the parameters β and r_c are adjusted to achieve the rapid convergence of the sum in (16) and force an agreement between the calculated and measured phonon frequencies.

We use Eqs. (8) and (23) in (16) and obtain the following expression for the electronic contribution to the phonon frequencies:

$$\omega_{q\rho}^2(E) = -\omega_{p1}^2\left(\sum_G \frac{[\vec{e}_{q\rho}\cdot(\vec{q}+\vec{G})]^2}{|\vec{q}+\vec{G}|^2} F(\vec{q}+\vec{G}) - \sum_{G\neq 0} \frac{[\vec{e}_{q\rho}\cdot\vec{G}]^2}{|\vec{G}|^2} F(\vec{G})\right) \ , \quad (24)$$

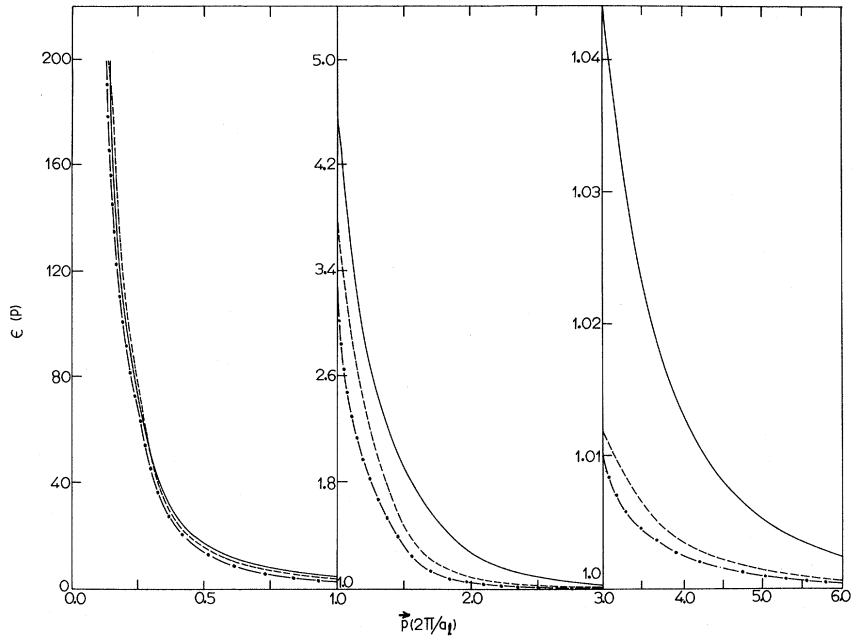

FIG. 1. Comparison of dielectric functions for the configuration $(3d)^9(4s)^1$. The dashed line represents the averaged isotropic dielectric function obtained from I and the solid line represents the lease-squares-fitted dielectric function. Dash-dotted line represents the dielectric function for the isotropic two-band model. Here p is measured in units of $2\pi/a_l$ while a_l is lattice parameter in Bohr units.

where

$$F(\vec{q}+\vec{G}) = \left(1 - \frac{1}{\epsilon(\vec{q}+\vec{G})}\right)\left(-1 + \frac{|\vec{q}+\vec{G}|^2}{4\pi Z e^2}\frac{1}{[1+(|\vec{q}+\vec{G}|r_c)^2]^2}\right)^2 , \tag{25}$$

$$\omega_{pl}^2 = 4\pi Z^2 e^2/M\Omega_0 . \tag{26}$$

III. CALCULATIONS AND RESULTS

We calculate the phonon frequencies of nickel in the paramagnetic phase. The contribution due to direct ion-ion interaction to the phonon frequencies is tabulated by Vosko *et al.*[18] for an fcc lattice in units of the plasma frequency ω_{pl}. We use their tabulation for the phonon wave vectors along the three principal symmetry directions [100], [110], and [111]. The electronic contribution is calculated with the help of Eq. (24). The dielectric function calculated with the help of Eq. (22) for the configuration $(3d)^9$ $(4s)^1$ is displayed in Fig. 1. In the low-$\vec{p}$ region, this dielectric function has very high values as compared with the case of simple metals. This is because of strong screening due to the d electrons.

We also tried to search for a simple analytic form for the dielectric function (17). We averaged the values of the dielectric function calculated in I for $\vec{p}$ along three principal symmetry directions by Houston's method. This averaged isotropic dielectric function is fitted to the following function:

$$\epsilon(p) = 1 + \frac{A}{p^2}\left(1 + \frac{4k_{Fs}^2 - p^2}{4k_{Fs}p}\ln\left|\frac{2k_{Fs}+p}{2k_{Fs}-p}\right|\right)$$

$$+\sum_m \frac{B_m}{p^2}\left(1 + \frac{4k_{Fdm}^2 - p^2}{4k_{Fdm}p}\ln\left|\frac{2k_{Fdm}+p}{2k_{Fdm}-p}\right|\right) , \tag{27}$$

where the coefficients A and B_m (which are independent of p) are determined by the method of the least squares. The averaged isotropic dielectric function (27) for the configuration $(3d)^9$ $(4s)^1$ is also shown in Fig. 1. We find that the dielectric function given by (22) is in better qualitative agreement with the averaged dielectric function than $\epsilon(\vec{p})$ given by (27).

The sum over $\vec{G}$ in (24) is taken for 259 nearest reciprocal-lattice vectors and the parameters β and r_c are adjusted in such a manner that the function $F(\vec{p})$ vanishes within the range of summation over $\vec{G}$. We first introduce some arbitrary values of β and r_c, then for a β, we scan a range of values of r_c and find that $r_c = 0.3$ is quite suitable. Next for this value of r_c, we scan a range of β and find that $\beta = 16.0$ yields the over-all best agreement with experimental measurements of Birgeneau *et al.*[19] The calculated phonon frequencies with these values of β and r_c are shown for the configuration $(3d)^9$ $(4s)^1$ by solid lines in Figs. 2–4 along [100], [111], and [110] directions, respectively. The other parameters and the physical

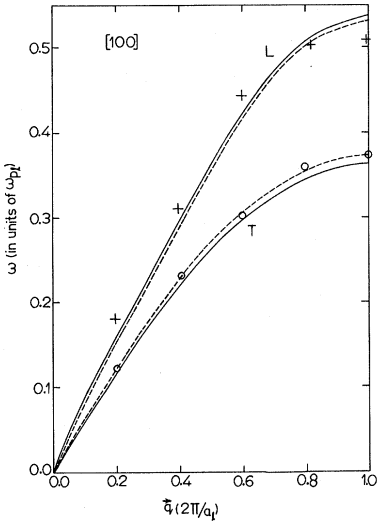

FIG. 2. ω vs $\vec{q}$ along [100] direction for nickel. Solid lines are for the configuration $(3d)^9(4s)^1$, while dashed lines are for the configuration $(3d)^{9.4}(4s)^{0.6}$. + and ○ denote the experimental measurements along longitudinal (L) and transverse (T) branches, respectively.

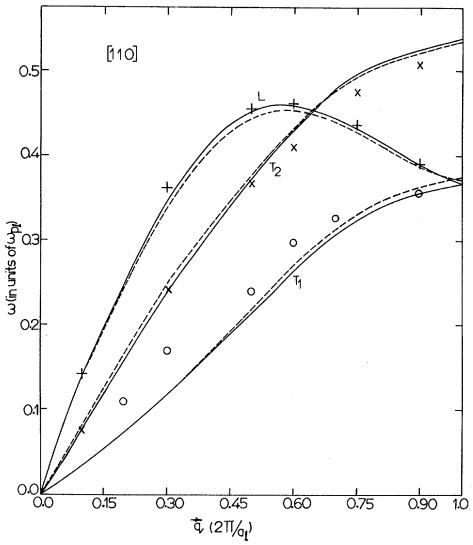

FIG. 4. ω vs $\vec{q}$ along [110] direction for nickel. The description of the figure is the same as for Fig. 2 except that here ○ and × denote the experimental phonon frequencies for the T_1 and T_2 branches, respectively.

constants are the same as used in I. For the same values of β and r_c, the calculations are repeated for the configuration $(3d)^{9.4}(4s)^{0.6}$. These results are shown by the dashed lines in the Figs. 2–4. The functions $F(\vec{p})$ for both configurations are displayed in Fig. 5 and tabulated in Table I for a set of values of $\vec{p}$.

In order to see how crucial the isotropic two-band model dielectric function is to our calculation, we calculated the phonon frequencies of Ni by using a free-electron Hartree dielectric function for the case of two conduction electrons per atom. We find that the calculated phonon frequencies manifest quite an erratic variation with $\vec{q}$, in spite of many attempts to adjust the values of the parameters β and r_c to give the best fit with experimental data. This indicates that the usual free-electron solutions for electronic screening are not tenable for transition metals, and one has to take into account the nature of d electrons.

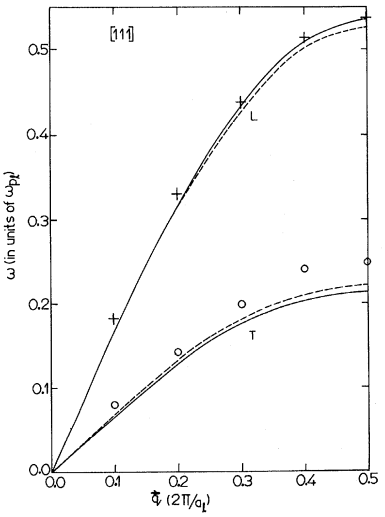

FIG. 3. ω vs $\vec{q}$ along [111] direction for nickel. The description of the figure is the same as for Fig. 2.

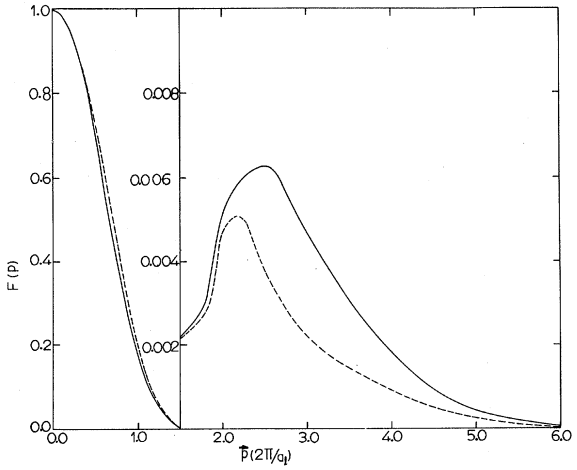

FIG. 5. Function $F(p)$: Solid line is for the configuration $(3d)^9(4s)^1$ while the dashed line is for the configuration $(3d)^{9.4}(4s)^{0.6}$. For $p > 1.5$, the function $F(p)$ is shown in the magnified scale in the right-hand side.

TABLE I. The function $F(p)$, where $\vec{p}$ is the reciprocal vector in units of $2\pi/a_l$ where a_l is the lattice parameter in Bohr units.

$\lvert\vec{p}\rvert$	$F(p)[(3d)^9(4s)^1]$	$F(p)[(3d)^{9.4}(4s)^{0.6}]$
0.1	0.986 56	0.986 97
0.4	0.799 96	0.805 46
0.6	0.592 46	0.601 89
0.8	0.372 02	0.382 51
1.0	0.186 46	0.193 92
1.2	0.066 05	0.068 76
1.5	0.002 27	0.002 23
1.8	0.002 97	0.002 75
2.0	0.006 19	0.004 71
2.5	0.007 33	0.003 65
3.0	0.005 20	0.002 20
3.5	0.003 21	0.001 45
4.0	0.001 81	0.000 91
4.5	0.000 95	0.000 52
5.0	0.000 46	0.000 27
5.5	0.000 21	0.000 12
6.0	0.000 09	0.000 05

IV. DISCUSSION

The model that we have used presents too simplified a picture of transition metals. Though the noninteracting band model is based on the detailed band-structure calculations, we did not consider explicitly the s-d hybridization which splits s and d bands in a transition metal. We neglected the exchange and correlation effects which should be quite important in transition metals. These effects can be grafted in an approximation commonly used for simple metals.[20] In a study of the ferromagnetic transition metals we shall have to consider a spin-dependent problem.

The separation between the core and the conduction electrons that we assumed in the model is not realistic. A core limited to a $(3d)^8$ configuration will be highly polarizable and we did not consider the polarization of the core. In order to extend this method of separating the core and the conduction electrons, one will have to know in detail the band structure of the metal. It should be possible to construct similar models for other transition metals if we have sufficient knowledge about their energy bands. We have incorporated in this model the effect of mutual orthogonalization of s- and d-electron wave functions and their orthogonalization to the core wave functions in a phenomenological way. A rigorous formulation will result in a very complicated form for the dielectric function. The nonlocality and energy dependence are essential features of the pseudopotentials for d bands. We used a local pseudopotential only as an extreme simplification and this point needs further investigation.

The calculated phonon frequencies of Ni for the configuration $(3d)^9(4s)^1$ and $(3d)^{9.4}(4s)^{0.6}$ differ at the most by 3%. The phonon frequencies for the longitudinal modes are lower for the configuration $(3d)^{9.4}(4s)^{0.6}$ than the corresponding frequencies for the configuration $(3d)^9(4s)^1$. Except for the T_2 branch in the [110] direction in the low-$\vec{q}$ region, this trend is reversed in the transverse branches. The agreement between the calculated and the experimental phonon frequencies is not very satisfactory for the T branch in the [111] direction in the high-$\vec{q}$ region and for the T_2 and T_1 branches in the [110] direction in the low-$\vec{q}$ region. The maximum deviation between the calculated and the observed frequencies is 25% in the T_1 branch in the [110] direction. We should also remember that the phonon frequencies measured at room temperature are for the ferromagnetic phase while our calculations are for the paramagnetic phase of Ni. The important point to be emphasized is that it is necessary to recognize the s and d natures of electrons in the problem of lattice dynamics of transition metals. We have shown that the ordinary free-electron formulas do not work.

ACKNOWLEDGMENT

The authors acknowledge the financial support from the Department of Atomic Energy, Government of India.

[1]S. K. Joshi and A. K. Rajagopal, Solid State Phys. 22, 159 (1968).

[2]L. J. Sham, Phys. Rev. 188, 1431 (1969).

[3]R. M. Pick, M. H. Cohen, and R. M. Martin, Phys. Rev. B 1, 910 (1970).

[4]J. U. Koppel, Ph. D. thesis (University of California, San Diego, 1968) (unpublished).

[5]J. G. Hanus, MIT Solid State and Molecular Theory Group Quarterly Progress Report No. 44, 1962, p. 29 (unpublished); L. F. Mattheiss, Phys. Rev. 134, A970 (1964); J. Yamashita, M. Fukuchi, and S. Wakog, J. Phys. Soc. Japan 18, 999 (1963); 19, 1342 (1964); S. Wakoh, *ibid.* 20, 1894 (1965); L. Hodges, H. Ehrenreich, and N. D. Lang, Phys. Rev. 152, 505 (1966); J. W. D. Connolly, *ibid.* 159, 415 (1967).

[6]W. A. Harrison, Phys. Rev. 181, 1036 (1969).

[7]S. K. Sinha, Phys. Rev. 169, 477 (1968).

[8]D. C. Golibersuch, Phys. Rev. 157, 532 (1967).

[9]S. Prakash and S. K. Joshi, Phys. Rev. B 2, 915 (1970).

[10]P. P. Ewald, Ann. Physik 64, 253 (1921); E. W. Kellerman, Phil. Trans. Roy. Soc. London A238, 513 (1940).

[11]L. J. Sham and J. M. Ziman, Solid State Phys. 15, 221 (1963).

[12]L. Liu and D. Brust, Phys. Rev. 173, 777 (1968); E. Hayashi and M. Shimizu, J. Phys. Soc. Japan 26, 1396 (1969); 27, 43 (1969).

[13]S. Prakash and S. K. Joshi, Phys. Rev. 187, 808

(1969).
[14]S. Prakash and S. K. Joshi, Phys. Letters 30A, 138 (1969).
[15]W. Kohn and L. J. Sham, Phys. Rev. 140, A1133 (1965).
[16]J. E. Robinson, F. Bassani, R. S. Knox, and J. R. Schrieffer, Phys. Rev. Letters 9, 215 (1962).
[17]W. A. Harrison, *Pseudopotentials in the Theory of Metals* (Benjamin, New York, 1966).
[18]S. H. Vosko, R. Taylor, and G. H. Keech, Can. J. Phys. 43, 1187 (1965).
[19]R. J. Birgeneau, J. Cordes, G. Dolling, and A. D. W. Woods, Phys. Rev. 136, A1359 (1964).
[20]S. Prakash and S. K. Joshi, Phys. Rev. 185, 915 (1969).

PHYSICAL REVIEW B VOLUME 4, NUMBER 6 15 SEPTEMBER 1971

Soft-X-Ray $L_{2,3}$ Spectrum and Electronic Band Structure of Chromium

David W. Fischer
Air Force Materials Laboratory, Wright-Patterson Air Force Base, Ohio 45433
(Received 8 March 1971)

The soft-x-ray $L_{2,3}$ emission and absorption spectra from pure chromium are shown and the effects of satellite emission and self-absorption are assessed. Features of the L_3 spectrum are discussed in terms of the energy-band structure. Results are evaluated by comparing the L_3 spectrum with the x-ray K and M spectra, with ultraviolet photoemission measurements, and with band-structure calculations. There is good agreement between theory and experiment as to the width of the occupied states, the position of the Fermi energy, and the position of most maxima and minima in both the occupied and vacant portions of the density of states. Some disparities are also observed but they involve primarily the fine features of the structure.

I. INTRODUCTION

The use of soft-x-ray spectra (SXS) for studying the band structure of 3*d* transition metals has been discussed in many publications over the last 35 years or so. Until quite recently, in fact, SXS was the only readily available experimental method of probing the structure as far as 5–10 eV below the Fermi energy (E_F). The last several years, however, have witnessed the growth and development of some new deep-band techniques such as ultraviolet photoemission spectroscopy[1] (UPS), ion-neutralization spectroscopy[2] (INS), and x-ray photoemission spectroscopy[3] (XPS). Each of these techniques has certain advantages in specialized cases, and each is capable of providing information related to the density of states of the material being studied. *None* of them, however, gives a direct picture of the density of states. Although these techniques all involve different types of electronic transitions and transtion probabilities, it can be quite instructive to compare the SXS, UPS, INS, and XPS results with each other and with theoretical calculations as has been done for Ni and Cu.[4,5] One can realistically expect to obtain reasonably good agreements as to the position of the Fermi energy, the width of the occupied states, and the position of the main maxima in each of the curves. Such agreements can lend confidence to both the experimental techniques and the theoretical computations of the band structure.

To date, the bulk of experimental and theoretical work performed on the 3*d* metals has been concentrated on the heavier members of the series: Fe, Co, Ni, and Cu. Little has been done on the lighter elements Ti, V, and Cr. This author has previously published the SXS $L_{2,3}$ spectra of Ti[6] and V[7] and Eastman has shown their UPS curves.[8] So far, however, no INS or XPS data has appeared for these elements. The purpose of this paper is to show recently obtained SXS data for Cr and relate them to the SXS results for Ti and V, to the UPS results, and to the available theoretical calculations. Points of agreement and disagreement in the comparisons will be discussed.

Of all of the deep-band experimental techniques mentioned above, SXS can supply more total information about the band structures of the transition metals than any one of the other techniques. Not only can one obtain data about the occupied band states by using emission spectra, but valuable information about the unoccupied states can be found in the absorption spectra. The other techniques (UPS, INS, and XPS) do not readily yield data on the normally unoccupied states. Furthermore, the x-ray results are capable of differentiating between the various wave symmetries admixed into the valence/conduction band. The K spectrum, for instance, reflects only the distribution of p symmetry in the band, while the $L_{2,3}$ and $M_{2,3}$ spectra reflect the distribution of s and d symmetry.

It is the s and d states which are of primary in-